ELSEVIER

Journal of Nuclear Materials 313–316 (2003) 429–433

journal of nuclear materials

www.elsevier.com/locate/jnucmat

Characterisation of deposited hydrocarbon layers below the divertor and in the pumping ducts of ASDEX Upgrade

M. Mayer *, V. Rohde, A. von Keudell, ASDEX Upgrade Team

EURATOM Association, Max-Planck-Institut für Plasmaphysik, Boltzmannstr. 2, D-85748 Garching, Germany

Abstract

The growth of codeposited layers has been studied with long term samples below the divertor IIb and in a pump duct of ASDEX Upgrade from March to August 2001. The composition of redeposited layers and their optical properties were analyzed with ion beam techniques and ellipsometry. The deposition in the sub-divertor area showed a complicated deposition pattern with a maximum deposition of about 1.3 μm. All deposits form soft hydrocarbon layers which consist mainly of deuterium and carbon with D/C from 0.7 to 1.4. Only a small deposition was observed in the pump duct, with a maximum of about 2.5×10^{15} D-atoms/cm^2 at the duct entrance. The observed deposition pattern in the duct is compared with simulation calculations assuming neutral hydrocarbon radicals as precursors for film deposition. The deposition pattern can be explained by two different radical species with surface loss probabilities $\beta < 10^{-3}$ and $0.1 \leqslant \beta \leqslant 0.9$. The most likely species are CD_3, C_2D_5 and C_2D_3 radicals.

Keywords: Redeposition; a-C:D; ASDEX-Upgrade; Co-deposition; Hydrocarbon radicals; Deuterium inventory

1. Introduction

The major disadvantage of carbon as a first wall material in a fusion device is the trapping of hydrogen isotopes by codeposition with eroded carbon atoms [1]. Tritium trapped in these codeposited layers will contain a significant amount of the total tritium inventory of a nuclear fusion reactor [2–4]. These layers can be formed even in areas without direct plasma contact, such as the louvres in the JET Mark IIA divertor [5], the area below the divertor II of ASDEX Upgrade [6], or the pump ducts of TEXTOR [1,7]. These areas can be reached only by neutral particles and not by ions, because only they can traverse the magnetic field lines. It has been shown in laboratory low temperature plasma experiments, that neutral hydrocarbon radicals such as CH_3, C_2H and C_2H_3 can contribute strongly to the growth of amorphous hydrogenated carbon layers [8,9], and it has been assumed that hydrocarbon radicals are responsible for the formation of layers in remote areas of nuclear fusion experiments [9]. These radicals can be formed either in the divertor plasma from the dissociation of stable CD_4 or C_2D_x ($x = 2, 4, 6$) molecules, which are present as chemical erosion products of carbon components, or they can be produced at the carbon divertor plates as results of chemical erosion processes or thermal decomposition of redeposited layers.

Reactive species hitting a wall may either adsorb with a sticking probability s, can react at the surface to form a non-reactive volatile molecule (for example CD_3 to CD_4) with probability γ, or they can be reflected with reflection probability r. The surface loss probability β, which is the probability of losing a reactive particle in a surface collision, is given by

$$\beta = s + \gamma \tag{1}$$

with $r + s + \gamma = 1$. The surface loss probability β can be determined with the cavity technique [9], and has been

* Corresponding author. Tel.: +49-89 3299 1637; fax: +49-89 3299 2279.

E-mail address: matej.mayer@ipp.mpg.de (M. Mayer).

0022-3115/03/$ - see front matter
PII: S0022-3115(02)01407-1

measured for several hydrocarbon radical species [8–10]. The surface loss probability can be astonishingly low: For CH_3 and C_2H_5 it is $<10^{-3}$ [8,11]. The surface loss probability is also an upper bound for the sticking coefficient s, which has been measured only for CH_3 radicals [11]. These low loss probabilities allow the penetration of hydrocarbon radicals to areas far away from their place of origin, where they can form hydrogen rich layers.

In this paper we describe the properties of layers which are deposited below the divertor and in the pump ducts of ASDEX Upgrade. The layer thickness distribution in the pump duct allows to test the hypothesis of hydrocarbon radicals as neutral precursors for film growth and the identification of the radical species.

2. Experimental

Silicon wafers were used as deposition monitors. They were installed below the roof baffle of divertor IIb and in the pump duct of segment 12. The samples were exposed from March to August 2001 for 461 plasma discharges (discharges #14130–14590) with a total discharge time in divertor configuration of 1424 s. The samples were at room temperature.

Deposited layers were analyzed with different ion beam analysis techniques:

- D was detected by nuclear reaction analysis (NRA) with incident 800 and 1200 keV ^{3}He ions. The protons from the D(^{3}He,p)α reaction were detected with a large angle proton counter covered by a 0.1 mm stainless steel foil.
- H was measured by elastic recoil detection analysis with incident 3 MeV ^{4}He ions at a recoil angle of 30°. The detector is covered by a 5 μm Ni foil and has a solid angle of 9.7×10^{-4} sr. Non-Rutherford recoil cross sections from [12,13] were used for spectrum evaluation.
- C and O were measured with RBS using 1.5 MeV incident protons at a scattering angle of 165°. The detector has a solid angle of 1.14×10^{-3} sr. Non-Rutherford scattering cross sections from [14] were used.

All spectra were evaluated with the program SIMNRA [15,16].

3. Computer simulation

A computer code STICKY has been developed, which allows to calculate the deposition profile of hydrocarbon radicals in a circular tube. STICKY is a Monte-Carlo code which follows individual particles until they either stick on the wall or leave the tube. The code assumes the following:

(1) Fully 3-dimensional treatment of particle trajectories in a tube with circular profile.
(2) Particles enter (and may leave) the tube from one side, the other tube end is either open or close.
(3) Particles enter the tube equipartitioned over the tube entrance area. The initial velocity components are distributed according to a solid angle weighted cosine distribution.
(4) If particles hit a tube wall, they can either stick, or they can be reflected. Particles are reflected with a solid angle weighted cosine distribution, i.e. $p(\theta) \propto \sin\theta\cos\theta$, where θ is the angle towards the surface normal. The random number generator creating this distribution is obtained from $\theta = \arcsin(\sqrt{x})$, where x is a random number equally distributed in $[0 \ldots 1]$.

The tube pressure is in the range 10^{-5}–10^{-3} mbar, resulting in free path lengths of 80–0.8 cm. At the higher pressures collisions with gas molecules in the tube have to be taken into account. This is done in the following way:

(1) The tube is filled with D_2 gas at a temperature of 293 K and pressure p. The product of radical mean free path $\bar{\lambda}$ and pressure is assumed to be 8.2×10^{-5} m mbar, corresponding to a radical molecule radius of 1.5 Å.
(2) During each step the free flight path λ of the radical molecule is obtained from $p(\lambda) = \exp(-\lambda/\bar{\lambda})$. The random number generator for this distribution is given by $\lambda = -\bar{\lambda}\ln(1-x)$, where x is a random number equally distributed in $[0 \ldots 1]$.
(3) At the end of the free flight path the radical collides with a D_2 molecule. The radical and the D_2 molecule have velocities according to the Maxwell–Boltzmann distribution. We assume a hard ball potential between the two molecules, and the scattering angle φ is given in the center of mass system by $\varphi(b) = \arccos(b/(r_1 + r_2))$, where b is the impact parameter, $r_1 = 1.1$ Å the radius of the D_2 molecule, and $r_2 = 1.5$ Å the assumed radius of the radical molecule. The radical mass is either 18 amu (CD_3) or 30 amu (C_2D_3). The probability distribution $p(b)$ for the impact parameter b is given by $p(b) = 2b/R^2$, where $R = r_1 + r_2$ and $0 \leqslant b \leqslant R$. This is the probability to hit a circular disk at radius b.

4. Results and discussion

4.1. Sub-divertor area

The positions of samples in the sub-divertor area are shown in Fig. 1.

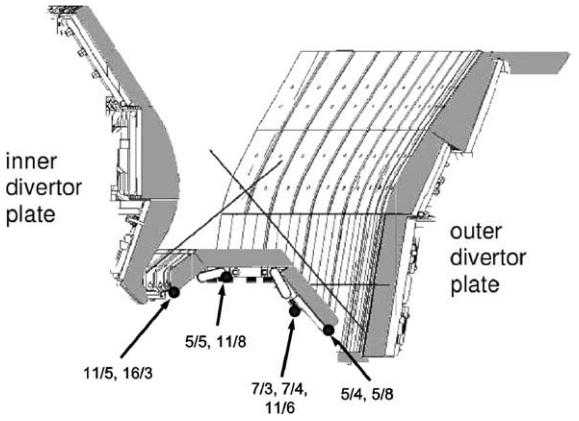

Fig. 1. Locations of long term samples in the divertor IIb of ASDEX Upgrade.

The properties of the deposited layers are summarized in Table 1. Samples oriented perpendicular to the magnetic field were looking in toroidal direction, with one sample in electron- and the other sample in ion direction. Layer thickness differences up to 30% were observed between the two samples, but showed no systematic trend. The thicknesses of the deposits depend on the distance to the strike point, where erosion takes place. This is visible in the outer divertor on samples 5/4 and 5/8 compared to 11/6 and 7/4: The distance of samples 5/4 and 5/8 to the divertor plate is about 73 mm, resulting in a seven times thicker deposit than on samples 11/6 and 7/4, which are 128 mm away from the divertor plate. The deposition in the inner divertor is about 2.5 times larger than in the outer divertor. This inner–outer asymmetry is much smaller than the asymmetry observed at JET. Only thin deposits are observed under the dome. There is no significant difference between samples oriented parallel and perpendicular to the magnetic field. This is noteworthy, as a plasma is observed in the sub-divertor region [17], and shadows in magnetic field direction behind obstacles are sometimes visible, indicating that charged particles also play some role in layer deposition. However, at least at the positions of the samples charged particles do not have a significant influence on the deposited layers.

The layers consist mainly of D and C. Additionally some O at a concentration of 10–15 at.% is observed, which may come from storage of the samples in air after exposure. The D/C ratio ranges from 0.7 to 1.4. This indicates soft hydrocarbon layers, which is confirmed by the very low refraction index: hard layers with D/C around 0.4 have a refraction index of 2.2–2.4, while soft layers have a refraction index below 1.8. The layers were mechanically soft and could be scratched easily. In the previous divertor II, also brownish layers with a lower D/C ratio around 0.4 were observed [6]. This type of layers is not observed any more at the sample positions, although these brownish layers still can be found in some limited areas by visual inspection. But generally the spread of these layers has largely decreased.

H is present at varying amounts in the layers, ranging from 10^{16} to $>10^{18}$ at./cm^2 with a H/D ratio of 0.3–0.5. This ratio is much larger than the H/D ratio in the ASDEX Upgrade plasma, which is about 0.05–0.1, and there was no H-campaign during the exposure of the samples. The amount of H is correlated with the total layer thickness, indicating that the layers either take up additional hydrogen from humid air during storage or D is exchanged with H – the details of this process are still unclear [1]. Other elements, especially boron and metals such as Fe or W, were below the detection limit.

On the structures below the inner divertor about 1.5×10^{22} D-atoms were deposited, and about 1×10^{22} below the outer divertor. In total about 2.5×10^{22} D-atoms (83 mg) were deposited on the structure below the divertor IIb, which is 0.3% ($-0.2\% + 0.7\%$) of the total D input of 7.3×10^{24} D-atoms. The indicated error is quite large due to the complicated geometry below the divertor.

4.2. Pump duct

A cross section of the pump duct in Section 12 of ASDEX Upgrade is shown in Fig. 2. The duct is almost circular with a diameter of 266 mm and a length of 3500 mm, where it kinks by 90° towards the pump. The duct

Table 1
Properties of deposited layers below the divertor

Sample	Position	Orientation to magnetic field	Thickness of deposit (at./cm^2)	Ratio D/C	Refraction index
5/4, 5/8	Outer	Perpendicular	4×10^{18}	0.95	1.55
11/6, 7/4	Outer	Perpendicular	6×10^{17}	1.28	1.55
7/3	Outer	Parallel	8×10^{17}	1.38	1.6
11/8, 5/5	Dome	Perpendicular	$\approx 4 \times 10^{16}$	–	–
11/5, 16/3	Inner	Perpendicular	1×10^{19}	0.70	1.6

The refraction index is at 632.8 nm.

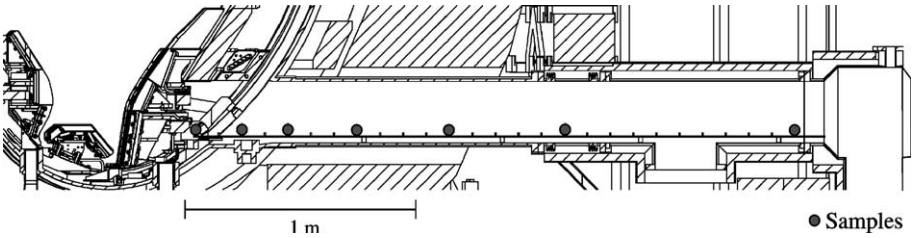

Fig. 2. Section of the pump duct in Section 12 of ASDEX Upgrade.

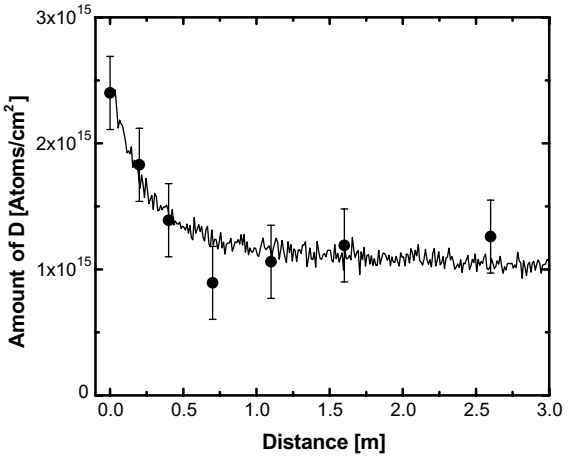

Fig. 3. Deposition of D in the pump duct of ASDEX Upgrade. Dots: Experimental data. Solid line: Monte-Carlo computer simulation assuming two different hydrocarbon radical species with surface loss probabilities $\beta = 0.3$ and $\beta = 0.0005$.

entrance is about 30 cm away from the inner divertor leg. The duct can be reached by gas from the divertor either by streaming through the sub-divertor area, or through narrow slits in the outer vertical target. Seven samples were mounted in the duct, the distribution of D on the samples is shown in Fig. 3. The deposition is small, with a maximum of about 2.5×10^{15} D-atoms/cm^2 close to the duct entrance. The deposition decreases towards the duct end to about 1.2×10^{15} D-atoms/cm^2. Additionally a constant amount of H at a level of 1.8×10^{16} atoms/cm^2 was observed. C and O were below the detection limit of about 5×10^{16} atoms/cm^2. The total amount of D deposited in the pump duct is about 4.1×10^{19} D-atoms, which gives a total amount of 5.7×10^{20} D-atoms (= 2 mg) in all 14 ducts of ASDEX Upgrade. As the total deuterium inlet was 7.3×10^{24} D-atoms during the whole discharge period, only a small fraction of about 8×10^{-5} gets trapped in the pump ducts.

The pump duct can be reached only by neutral particles, as it is oriented perpendicular to the magnetic field lines. The simulated deposition profile of hydrocarbon radicals, as calculated with the program STICKY, is shown in Fig. 3, assuming two radical species with surface loss probabilities $\beta = 5 \times 10^{-4}$ and $\beta = 0.30$. For Fig. 3 the pump duct pressure was assumed to be zero, i.e. collisions with D_2 molecules were not taken into account. The experimental data are well reproduced. Fit to the experimental data always requires at least two radical species, one with β in the range 0.1–0.9 (best fit is obtained for $\beta = 0.30$), and the other with $\beta < 10^{-3}$. β values in the range 10^{-3} to 0.1 can be excluded.

The mean pressure in the duct was 3.5×10^{-4} mbar during a discharge. The mean free path of hydrocarbon radicals at this pressure is about 24 cm, which is comparable to the diameter of the pump duct, and collisions with D_2 molecules in the duct can be neglected. But the pressure shows large variations with a maximum pressure of 4×10^{-3} mbar during some discharges, and at the higher pressures collisions with D_2 molecules play some role. Best fit to the experimental data is obtained for $\beta = 0.3$ at $p = 0$, which decreases to $\beta = 0.28$ at $p = 10^{-3}$ mbar and $\beta = 0.24$ at $p = 4 \times 10^{-3}$ mbar, with the possible range from 0.08 to 0.75. The influence of the duct pressure is therefore smaller than the inaccuracy of the measurement.

Surface loss probabilities β for different hydrocarbon radicals are known from laboratory experiments. They are $\beta < 10^{-3}$ for CH_3 and C_2H_5 [8], $\beta = 0.8$ for C_2H [8], and $\beta = 0.35$ for C_2H_3 [8]. From the D-distribution in the pump duct of ASDEX Upgrade we get at least two radical species with $\beta < 10^{-3}$ and $0.1 \leqslant \beta \leqslant 0.9$. The most likely candidates are therefore CD_3 and C_2D_5 as low sticking species and C_2D_3 as higher sticking species, though C_2D also may play some role.

5. Conclusions

The growth of codeposited layers below the divertor IIb and in a pump duct of ASDEX Upgrade has been studied from March to August 2001. At all areas soft hydrocarbon layers with a ratio D/C ranging from 0.7 to 1.4 are observed, the maximum deposition was 1.3 μm. The occurrence of brownish layers with a lower D/C ratio close to 0.4, which were observed in the previous

divertor II [6], has largely decreased. As these layers require ion impact to be formed, their decrease may be due to a decrease of the ion flux below the divertor.

The observed deposition pattern in the pump duct is compared with simulation calculations assuming neutral hydrocarbon radicals as precursors for film deposition. The deposition pattern can be explained by two different radical species with surface loss probabilities $\beta < 10^{-3}$ and $0.1 \leqslant \beta \leqslant 0.9$. The most likely species are C_2D_3, CD_3 and and C_2D_5 radicals. By this measurement, it has been shown for the first time in a nuclear fusion device that hydrocarbon layers are deposited by neutral hydrocarbon radicals. Although the deposition in the duct is small, the same species will also be present in other areas below the divertor. This is confirmed by the identical deposition on areas below the divertor which are oriented parallel and perpendicular to the magnetic field. This can be explained only if the layers are deposited by neutral particles. The hydrocarbon radicals are formed either in the divertor plasma from the dissociation of stable CD_4 or C_2D_x ($x = 2, 4, 6$) molecules, which are present as chemical erosion products of carbon components, they can be formed in the low temperature plasma which is observed below the roof baffle [17], or they can be produced at the divertor plates as results of chemical erosion processes or thermal decomposition of redeposited layers. The source of the radicals requires further investigation.

Acknowledgement

Ellipsometry measurements were performed by T. Schwarz-Selinger, whose help is gratefully acknowledged.

References

[1] M. Mayer, V. Philipps, P. Wienhold, H.G. Esser, J. von Seggern, M. Rubel, J. Nucl. Mater. 290–293 (2001) 381.
[2] G. Federici, R. Anderl, J.N. Brooks, R. Causey, J.P. Coad, D. Cowgill, R. Doerner, A.A. Haasz, G. Longhurst, S. Luckhardt, D. Mueller, A. Peacock, M. Pick, C. Skinner, W. Wampler, K. Wilson, C. Wong, C. Wu, D. Youchison, Fusion Eng. Des. 39&40 (1998) 445.
[3] G. Federici, R. Anderl, P. Andrew, J.N. Brooks, R.A. Causey, J.P. Coad, D. Cowgill, R.P. Doerner, A.A. Haasz, G. Janeschitz, W. Jacob, G.R. Longhurst, R. Nygren, A. Peacock, M.A. Pick, V. Philipps, J. Roth, C.H. Skinner, W.R. Wampler, J. Nucl. Mater. 266–269 (1998) 14.
[4] G. Federici, J.N. Brooks, D.P. Coster, G. Janeschitz, A. Kukuskhin, A. Loarte, H.D. Pacher, J. Stober, C.H. Wu, J. Nucl. Mater. 290–293 (2001) 260.
[5] J.P. Coad, N. Bekris, J.D. Elder, S.K. Erents, D.E. Hole, K.D. Lawson, G.F. Matthews, R.-D. Penzhorn, P.C. Stangeby, J. Nucl. Mater. 290–293 (2001) 224.
[6] V. Rohde, H. Maier, K. Krieger, R. Neu, J. Perchermaier, and ASDEX Upgrade Team, J. Nucl. Mater. 290–293 (2001) 317.
[7] J. von Seggern, P. Wienhold, T. Hirai, V. Philipps, Long term behaviour of material erosion and deposition on the vessel wall and remote areas of TEXTOR-94, these Proceedings.
[8] C. Hopf, T. Schwarz-Selinger, W. Jacob, A. von Keudell, J. Appl. Phys. 87 (6) (2000) 2719.
[9] A. von Keudell, C. Hopf, T. Schwarz-Selinger, W. Jacob, Nucl. Fusion 39 (10) (1999) 1451.
[10] C. Hopf, K. Letourneur, W. Jacob, T. Schwarz-Selinger, A. von Keudell, Appl. Phys. Lett. 74 (25) (1999) 3800.
[11] A. von Keudell, T. Schwarz-Selinger, W. Jacob, J. Appl. Phys. 89 (5) (2001) 2979.
[12] J.E.E. Baglin, A.J. Kellog, M.A. Crockett, A.H. Shih, Nucl. Instrum. and Meth. B 64 (1992) 469.
[13] A.J. Kellog, J.E.E. Baglin, Nucl. Instrum. and Meth. B 79 (1993) 493.
[14] R. Amirikas, D.N. Jamieson, S.P. Dooley, Nucl. Instrum. and Meth. B 77 (1993) 110.
[15] M. Mayer. SIMNRA user's guide, Tech. Rep. IPP 9/113, Max-Planck-Institut für Plasmaphysik, Garching, 1997.
[16] M. Mayer, in: J.L. Duggan, I. Morgan (Eds.), Proceedings of the 15th International Conference on the Application of Accelerators in Research and Industry, AIP Conference Proceedings, vol. 475, American Institute of Physics, 1999, p. 541.
[17] V. Rohde, M. Mayer, J. Neuhauser, ASDEX Upgrade Team. On the formation of a-C:D layers and parasitic plasma underneath the roof baffle of the ASDEX Upgrade divertor, these Proceedings.